Tanker UAV for Autonomous Aerial Refueling

Jesús Martín, Hania Angelina, Guillermo Heredia and Aníbal Ollero

Abstract Increasing flight endurance of Unmanned Aerial Vehicles (UAVs) is a main issue for many applications of these aircrafts. This paper deals with air to air refueling between UAVs. Relative estimation using only INS/GPS system is not sufficiently accurate to accomplish an autonomous dock for aerial refueling using a boom system in the tanker.

In this paper we propose a quaternion based relative state estimator to fuse GPS and INS sensor data of each UAV with vision pose estimation of the receiver obtained from the tanker. Simulated results validate the approach and are the starting point for ground and flight tests in the next months.

Keywords UAV · Refueling · Formation flight · Boom

1 Introduction

In aerial refueling, there are two commonly used methods: the probe and drogue refueling system and the boom and receptacle refueling system [1]. In each case, the operation procedure is different. Firstly, in the probe and drogue method, the tanker aircraft acts as a passive element releasing a long flexible hose that trails behind and below the plane through which the fuel flows. At the end of the hose there is a cone-shaped component, where the receiver is hooked, known as a drogue or basket. The receiver aircraft extends a device called a probe, which is a

J. Martín(✉) · G. Heredia · A. Ollero
Robotics, Vision and Control Group, University of Seville, Seville, Spain
e-mail: {jesus.martin,guiller,aollero}@us.es

H. Angelina
Airbus Defence and Space, Madrid, Spain
e-mail: hania.angelina@airbus.com

A. Ollero—This work has been supported by Airbus Defence & Space under the project Open Innovation SAVIER and the MarineUAS PROJECT (H2020-ITN-642153).

L.P. Reis et al. (eds.), *Robot 2015: Second Iberian Robotics Conference*,
Advances in Intelligent Systems and Computing 417,
DOI: 10.1007/978-3-319-27146-0_44

rigid arm placed usually on one side of the airplane. As the tanker flies in a racetrack, with no control on the drogue, the receiver aircraft flies behind and below the tanker aircraft and so that the probe of the receiver aircraft docks with the drogue from the tanker. Once the docking is accomplished, fuel is pumped through the hose, and the two aircrafts fly in formation until the fuel transfer is complete. Once the refueling is completed, the receiver aircraft then decelerates to undock the probe out of the drogue.

In the boom and receptacle refueling method, the approach change. Here the tanker is an active part in the refueling maneuver due to the possibility of boom position control. The boom can be assimilated to a long, rigid tube, fitted to the rear of the tanker aircraft. It normally has three degrees of freedom: pitch, yaw and a telescoping extension. Small wings enable the boom to be controlled into a receptacle of the receiver aircraft. The receiver aircraft is equipped with a receiver socket fitted onto the top of the aircraft, on its center line and usually either behind or close to the front of the cockpit. The receiver socket connects to the aircraft fuel system to redistribute the fuel into the receiver tanks. The boom has a nozzle which docks into the socket. During refueling operations, the tanker aircraft flies in a racetrack and level attitude at constant speed, while the receiver takes different standards positions behind and below the tanker before reaching the contact one. As the receiver pilot flies in formation with the tanker, the boom operator in the tanker's tail uses a joystick to move the boom and extend the telescoping component to connect the boom's nozzle to the receiver. Once docked, an electrical signal is passed between the boom and receiver, the valves in both the boom and the receiver are opened. Pumps on the tanker drive fuel through the boom fuel pipeline and into the receiver. When refueling is complete, the valves are closed and the boom is retracted before the receiver break the formation.

Compared to boom based refueling system, drogue based is simpler and more flexible, can be implemented in multiple types of aircrafts, and allows multiple aircraft being refueled. However, the drogue provides a lower fuel transfer rate. In the drogue based system the docking maneuver are made by the receiver aircraft, which is a demanding task for the receiver pilot. In boom based system, the receiver pilot's workload is slightly lower. The boom based system was designed for USAF heavy bomber refueling due to the higher fuel transfer rate. However, the tanker can only service one receiving aircraft at a time. Furthermore, the space and weight associated with the boom assembly limit the types of aircraft that can be equipped with this system.

The aerial refueling maneuver is divided into three phases: the pre-refueling or approach phase, the refueling phase, and the separation phase. In the approach phase, the receiver aircraft approaches the tanker aircraft from below and behind and gets connected with the tanker. This phase is also divided in three steps: wing position, pre-contact and contact. During the refueling phase, fuel is pumped from the tanker aircraft into the receiver aircraft. The receiver aircraft tries to hold a stationary position relative to the tanker aircraft to maintain the connection between drogue and probe, or boom and receptacle. This phase can also be called "station keeping". The separation phase begins as soon as fuel transfer ends. The receiver aircraft decelerates and becomes detached from the tanker aircraft.

Tanker wake turbulence makes flying the receiver aircraft during aerial refueling, especially during the first two phases, more difficult than under normal flight. Furthermore, as the receiver aircraft approaches the tanker aircraft in drogue based system, the relative position of the hose and drogue fluctuates due to wind gusts and turbulence. Then, it is not a trivial task to make the connection between the drogue and the probe. For a manned aircraft, such difficulties can be overcome by a pilot's agility. For UAVs, these difficulties impose challenges that should resolved through appropriated automatic flight control system design.

The developing of aerial refueling requires advances in boom based system for many reasons [2] [3] including higher flow rates, lighter work load for the receiver pilot, simpler equipment for the receiver aircraft, insensitivity to perturbations, easier docking operation and possibility to automatize the tanker operation.

The system proposed in this paper is composed of an UAV with an autonomous boom, equipped with a computer vision system and a refueling computer.

The boom is designed with CATIA and XFLR5 CFD. Two control surfaces are installed in a "H" configuration on the back of the boom and are used to control the boom attitude in pitch and roll [3] [4].

Aerial refueling is a sustained close formation flight. Close formation flight is a problem that need an accurate relative state estimate and robust formation guidance that utilizes the estimated relative state of the tanker and receiver aircraft. The simplest method to obtain the relative positioning is to compare the GPS coordinates from the tanker to the receiver. This method is useful in high separation formation flight due to accuracy is in the order of meters, but it is not enough for aerial refueling. In addition to this error, a very important problem is the time synchronization error between the measurements of both UAVs. High horizontal vehicle dynamics and data losses increase this error.

Aerial refueling needs an accuracy of around 0,4 meters. In order to achieve this, directly observed measurements should be used. Computer vision techniques previously applied in formation flight include active visual contours [5] [6], silhouette based techniques [7] and feature extraction [8] [9]. On the other hand, the drawback of vision systems is the high influence of occlusion, incorrect matching, cluttering and dynamic lighting conditions. To compensate these drawbacks and develop a robustness and accurate aerial refueling estimator, it is necessary to use information from inertial sensor, magnetometers, GPS and barometer.

An unscented Kalman filter (UKF) is proposed for the on board AHRS (Attitude and heading reference system) of each UAV and the relative state estimation [10] [11]. Each UAV has a UKF based AHRS to fuse on board GPS, inertial sensors, magnetometer and barometer. Furthermore, on board of the tanker, refueling estimator use an UKF to fuse vision data, receiver state vector and measurements, and tanker state vector and measurements [12]. The unscented Kalman filter (UKF) has several advantages over the extended Kalman filter (EKF). The derivation of Jacobians is not necessary, provides at least second-order nonlinear approximation instead of the first-order EKF, is more robust to initial errors and computation requirements are almost the same. In the aerial refueling problem, initial errors are particularly important due to the large difference in accuracy between the GPS and vision-based measurements, hence the resilience of the filter to initial error is very important. A downside of the UKF is that a quaternion parametrization of the attitude results in a non-unit quaternion estimate when the mean is computed. In our case we use generalized Rodrigues parameters (GRPs) to represent the attitude error. In our system, receiver and tanker are flying in formation. Visual markers are in the receiver and the tanker has mounted a camera pointing backwards with 5º of negative pitch. The boom root is 10 centimeters down of the tanker center of gravity to minimize the effect of the boom movement in the tanker.

2 Problem Formulation of Relative Estimation in Tanker Frame

This section describes the complete relative estimation algorithm First, a review of state estimation of each individual UAV be done through a filter UKF, and subsequently extended this algorithm to estimate the relative between the tanker and receiver. Subsequently adding vision measures will be explained.

2.1 Problem Formulation of Relative Estimation in Tanker Frame

As in[11] an UKF based state estimator is used, the individual state estimation x is obtained by measurements fusion of the differents sensor of each UAV. This process is based in two steps, prediction and observation. During the prediction stage the UAV dynamic model is used to predict the next time step state vector. The inputs, u, are the angular rates provided by the three axis gyros and the acceleration provided by the three axis accelerometer in body axis. In the observation phase measurements from the GPS, three axis magnetometer and barometer are used to correct the estimate

$$x = [\, P\; V\; \boldsymbol{q}\; a\; a_b\; \omega_b]^T \tag{1}$$

$$u = \left[\tilde{a}_b\; \tilde{\omega}_{ib}^b\right]^T \tag{2}$$

where the position $P = [\, X\; Y\; Z]^T$ and velocity $V = [\, v_x\; v_y\;\; v_z]^T$ are expressed in the NED (north-east-down) navigation frame, using as origin the ground station position. The quaternion $\boldsymbol{q} = [\, q_0\; q_1\;\; q_2\; q_3]^T$ describes the aircraft attitude used to form the rotation matrix C_b^n, which is used to transform from body to navigation frame. The definition of C_b^n and all other inertial mechanisation equations, and a full derivation of the INS mechanisation equations can be found in [13]. In the state propagation, the following inertial navigation mechanisation equations are used

$$\dot{x} = \begin{bmatrix} \dot{P} \\ \dot{V} \\ \dot{q} \\ \dot{\omega_B} \\ \dot{a_b} \end{bmatrix} = \begin{bmatrix} V \\ C_b^n \tilde{a} - (2\omega_{ie}^n + \omega_{en}^n) \times V + g^E \\ \frac{1}{2} \tilde{\Omega}_{\tilde{\omega}} q \\ n_{\omega_b} \\ n_{a_b} \end{bmatrix} \quad (3)$$

where $\tilde{a}_b$ and $\tilde{\omega}_{ib}^b$ are the IMU accelerometer and gyro varying bias, g^e is the Earth gravity vector in the navigation frame and ω_{ie}^n is the rotation of Earth in the navigation frame [13]. It is assumed that the navigation frame is fixed, and therefore ω_{en}^n is a zero vector, a_b and ω_b are defined as a random walk where n_{ω_b} and n_{a_b} are zero-mean Gaussian random variables, $\tilde{a}$ and $\tilde{\omega}$ are the bias and noise corrected imu measurements, and n_a and n_ω are the accelerometer and gyro measurement noise terms. The gyro measurement are corrected by the Earth´s rotation.

In the state observation phase, the different sensor sampling rates have been taken into account. Thus, $h^{gps}[x,k]$ is used when GPS measurement is available whereas $h^{no\ gps}[x,k]$ is taken into account when the magnetometer and pressure observations are available.

Then,

$$h^{gps}[x,k] = \begin{bmatrix} \bar{P}^{gps} \\ \bar{V}^{gps} \end{bmatrix} = \begin{bmatrix} P^- + C_b^n r_{gps} + n_{P_{gps}} \\ V^- + C_b^n \tilde{\omega} \times r_{gps} + n_{V_{gps}} \end{bmatrix} \quad (4)$$

where r_{gps} is the position of the GPS antenna relative to the centre of gravity, $n_{P_{gps}}$ and $n_{V_{gps}}$ are the measurement noise terms for the GPS position and velocity.

Moreover,

$$h^{no\ gps}[x,k] = \begin{bmatrix} \bar{h} \\ \bar{\psi} \end{bmatrix} = \begin{bmatrix} h_0 - Z^- + n_h \\ \tan^{-1}\left(\frac{2(q_0 q_3 + q_1 q_2)}{1 - 2(q_2^2 + q_3^2)}\right) + n_\psi \end{bmatrix} \quad (5)$$

where n_h and n_ψ are the measurement noise terms of the pressure altitude and the heading.

Raw data sensor have to be preprocessed before use in the observation models presented previously. GPS measurements are in geodetic frame, and are converted in to the navigation frame using the transformation in [13]. Then, heading $\tilde{\psi}$ is calculated from the observed magnetic vector, $\tilde{H}$ by first de-rotating through roll, ϕ, and pitch, θ using (6) and (7) and then calculating $\tilde{\psi}$ using

$$\tilde{M}_x = \tilde{H}_x \cos\theta + \tilde{H}_y \sin\theta \cos\phi + \tilde{H}_z \cos\phi \sin\theta \quad (6)$$

$$\tilde{M}_y = \tilde{H}_y \cos\phi + \tilde{H}_z \sin\phi \quad (7)$$

$$\tilde{\psi} = atan2\left(-\tilde{M}_y, \tilde{M}_x\right) + \psi_{dec} \quad (8)$$

Altitude above mean sea level (MSL), $\tilde{h}$, is now calculated using the atmospheric pressure. First, the pressure at MSL, ρ_{MSL}, is estimated using

$$p_{MSL} = p_0 \left(1 - \frac{L\,h_0}{T_0}\right)^{\frac{-gM}{R\,L}} \tag{9}$$

where p_0 is the initial pressure and $h_o$is the initial MSL height, as observed by the GPS. Finally, $\tilde{h}$ is determined using

$$\tilde{h} = \frac{T_0}{L}\left(1 - \left(\frac{\tilde{p}}{p_{MSL}}\right)^{\frac{R\,L}{g\,M}}\right) \tag{10}$$

The equations of the prediction and update stage are omitted, but can be found in [10], [14], [15].

2.2 Estimation

This section describes the relative state estimation framework to be used in the tanker to estimate the receiver position, in a turbulent outdoor environment, with change in wind direction and intensity and with different and dynamic lighting conditions. Our approach employs computer vision to provide an additional measurement. In this way it is possible to provide an accurate and reliable state estimate which is capable to maintain the accuracy during transient visual outages, but degrades during extended outages. The relative state, $x_{r|t}$ contains the position $P_{r|t}$, the relative velocity $V_{r|t}$ and a pressure bias h_b. The state are expressed as the tanker with respect to the leader, in the navigation frame and centred on the tanker. h_b is estimated to account for bias in the measurement of the barometric altitude.

$$x_{r|t} = \left[\, P_{r|t}\; V_{r|t}\; h_b \right]^T \tag{11}$$

$$u_{l|f} = [\, \widetilde{a_r}\; q_r\; \tilde{a}_t\; q_t\; 0]^T \tag{12}$$

$$Q_{l|f} = diag\; [\sigma^2_{\widetilde{a_r}}\;\; \sigma^2_{qr}\;\; \sigma^2_{\widetilde{at}}\;\; \sigma^2_{qt}\; \sigma^2_{h_B}\,] \tag{13}$$

To avoid convergence problems to incorrect and ambiguous states, during vision updates, q_r and q_t have been excluded from $x_{r|t}$, q_r, and q_t is estimated in each aircraft and transmitted between both of them

$$\dot{x}_{r|t} = \begin{bmatrix} \dot{P}_{r|t} \\ \dot{V}_{r|t} \\ \dot{h}_B \end{bmatrix} = \begin{bmatrix} V_{r|t} \\ C^n_r \tilde{a}_r - C^n_t \tilde{a}_t \\ 0 \end{bmatrix} \tag{14}$$

As in the individual on board estimator described in the previous section, the relative UKF based refueling estimator uses of GPS measurements, positioning and velocities, and barometric altitude. Using individual absolute measurement increase the time synchronization between data samples, especially in the horizontal movements where the dynamics are faster. Receiver data is transmitted to tanker wirelessly, so latency should be taken into account. Milliseconds delays in data transmission involve meters of error in positioning.

In this work the problem of storing the tanker data with time stamp, is approached using TOW (time of week) of the GPS and then wait to the receiver data with an adequate TOW. All the measurements are delayed by communications latency, and therefore the error is a function of the latency and relative position dynamics.

In case of matching of the receiver and tanker GPS measurements the following relative estimator correction is applied

$$h^{gps}\left(x_{r|t}^{-}, k\right) = \begin{bmatrix} P_{r|t}^{-} \\ V_{r|t}^{-} \end{bmatrix} \tag{15}$$

Taking into account that the vertical relative velocity is low, the relative altitude corrections are applied each time step,

$$h\left(x_{r|t}^{-}, k\right) = -Z_{r|t}^{-} - h_b \tag{16}$$

2.3 Vision System

As in [11] our system uses a features based method where visual markers are in the receiver, in a known position. Receiver is observed by the tanker camera. It is critical that most of the markers can be seen during all the refueling maneuver. Pose can be calculated directly using the n correspondences between the markers position of the receiver ς_j^r, the 2D observations $\overline{\delta_j}$ and the camera parameters. This requires $n \geq 3$ for a solution and $n \geq 4$ for a unique solution. To solve this PnP problem we used POSIT [16]. The drawback of the of this vision system are the effects in the pose estimation of matching fails, occlusions or a partial part of the target outside of the FOV. These fails are very problematic during the approximation maneuver or the docking phase.

As in [11] we propose a tightly-coupled design with use the n raw 2D marker observations of the receiver, where $\tilde{\delta}_j = \left[u_j v_j \right]^T, j = 1, \dots, n$. To guarantee the observability in the UKF $n = 4$ and $n \geq 3$ is required [8] [17]. The expected observations $\bar{\delta}_j, j = 1, \dots, m$ are calculated firstly transforming ς_j^t from receiver´s body frame to the world frame, using 17.

$$\varsigma_j^t = C_n^t \left(C_r^n \varsigma_j^r + P_{r|t}\right) \tag{17}$$

Then, using (18), vision sensor extrinsic parameters transform ς_j^t to the camera frame

$$\varsigma_j^c = \begin{bmatrix} C_t^c & P_{t|c} \end{bmatrix} \begin{bmatrix} \varsigma_j^f \\ 1 \end{bmatrix} \tag{18}$$

Where $P_{t|c}$ and C_t^c are the translation and rotation from the followers body frame to the camera frame. C_t^c include the camera mounting Euler angles and the axes transformation. $\overline{\delta_J}$ is calculated using K, a matrix which encapsulates the camera intrinsic parameters, focal length, aspect ratio, principal point and distortion. The final vision measurement model is provided in (20).

$$\begin{bmatrix} \overline{\delta_J} \\ 1 \end{bmatrix} = K \begin{bmatrix} \frac{\varsigma_{x_j}^c}{\varsigma_{z_j}^c} \\ \frac{\varsigma_y^c}{\varsigma_{z_j}^c} \\ 1 \end{bmatrix} \tag{19}$$

$$h^{vis}\left(x_{\overline{r|t}}, k\right) = \begin{bmatrix} \bar{\delta}_1 & \bar{\delta}_2 & \dots & \bar{\delta}_n \end{bmatrix}^T \tag{20}$$

3 Refueling Boom Modelling

The refueling boon has three degrees of freedom, pitch, yaw and extension. In our case, extension can be neglected, so pitch angle (θ_{boom}) about the y axis and yaw angle (β_{boom}) have been considered for boom modeling. The boom is modeled in Simmechanics to create a coupled model of the tanker and the boom.

Fig. 1 GRVC Tanker & Boom prototype

In our boom two independent control surfaces are installed symmetrically to control in pitch and yaw angle independently, the wingspan of elevator are 650mm and the rudder are 110mm. During the refueling maneuver it is necessary an automatic control system to manipulate the boom via rudder and elevator. The objective of the automatic control is to maintain the adequate attitude to dock with the receiver UAV.

During the modelling of the system, the following assumptions are taken into account: boom mass is constant, fuel flow is neglected, moment of inertia are constant, the boom is stiff, the aerodynamics forces of boom are equally distributed, the application point is constant in all the flight envelope and the joints are friction free.

According to the two degree-of-freedom and the stiffener of the boom, the equation of motion are written in the form shown in (21) and (22).

$$M_{\boldsymbol{\theta}} = |L_{og}|(G_z - D\sin\theta_{boom}) - |L_{of}|L\cos\theta_{boom} = J_\theta\ddot{\theta} \tag{21}$$

$$M_\psi = |L_{og}|G_y\sin\theta_{boom} + Y|L_{of}|\sin\theta_{boom} = -J_\phi\ddot{\psi} \tag{22}$$

where L_{og} are the distance between joint and centre of gravity and L_{of} is the distance between the joint and the force application point. G_y and G_z are the gravity force, that can be decomposed into three directions in the boom body coordinate system, two of which are

$$G_y = mg\sin\psi \tag{23}$$

$$G_z = mg\cos\theta\cos\psi \tag{24}$$

Lift force consists of fixed-boom contribution, elevator contribution and extension-boom contribution, and are represented with L. Lateral force, Y, comes from the rudders, and drag force, D, from the whole boom.

$$L = \frac{1}{2}\rho S_e V_\infty^2 C_l \tag{25}$$

$$D = \frac{1}{2}\rho S_e V_\infty^2 C_{d0_e} + \frac{1}{2}\rho S_r V_\infty^2 C_{d0_r} \tag{26}$$

$$Y = \frac{1}{2}\rho S_r V_\infty^2 C_Y \tag{27}$$

When boom and receiver are docked, the boom movement obeys to the tanker and receiver relative movement. Boom is designed in CATIA V5 and the aerodynamics coefficients, such as lift, drag, and moment coefficients are calculated using XFLR5.

Our boom has an onboard controller with a 6 DOF IMU and analog angle sensor in the joint. Two methods of attitude estimation are developed, a direct read from the analog sensor in the joint, and with the on board IMU with a linear Kalman filter for the attitude estimation. Pitch and yaw command are calculated with the information obtained from the relative state estimator.

$$\theta_{cmd} = \tan^{-1}(X_{rel}/Z_{rel}) - \theta_{tanker} \tag{28}$$

$$\psi_{cmd} = \tan^{-1}(X_{rel}/y_{rel}) \tag{29}$$

Finally, a PID controller is used for attitude control of the boom, depending the angles references. This angles, depends of the boom flying phase, that are divided in deploy, operation and recovery of the boom.

4 Simulations

This section present a precise simulation environment to test different estimators and algorithms focused in aerial refueling. The Simulator provides a controllable environment to compare initial results prior to flight test. Tanker and receiver are modeled as a 6DOF non-linear system. The actuators are modeled with first order time lag, saturation limits and rate limits. The environment is modeled using earth gravity models, magnetic field models, winds and atmospherics models. UAV and boom sensor suite are modeled with bias, Gaussian noise and cross coupling. The GPS model also incorporates Gauss-Markov noise. Telemetry between tanker and receiver includes latency and the possibility of data packets loss.

Vision sensor was modeled with a resolution of 1920x1080 pixels and a FOV 70ºx42º at 30fps. FOV is an important parameter in camera selection, because the need of tracking all the markers during the refueling maneuver. To calculate relative pose, firstly requires simulate pixel coordinates. The coordinates were calculated using (17) to (19) and the position and attitudes of the tanker and the receiver. Then white noise and a random order in the pixel stream were added to simulate the simulated measurements.

Figure 2 and 3 represent the relative attitude and position between tanker and receiver respectively. The green one represents the true data obtained from the simulator, the red represents the raw data of each UAV, the intense blue represents the vision measurements and the light blue the estimated data.

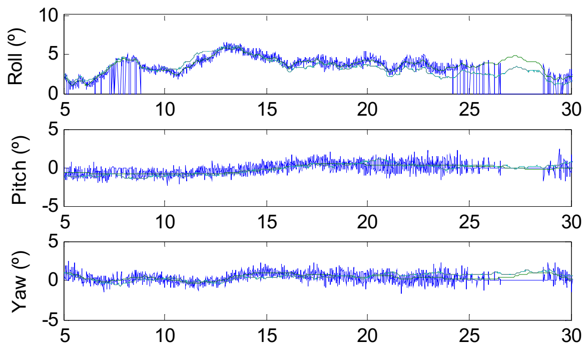

Fig. 2 Relative attitude

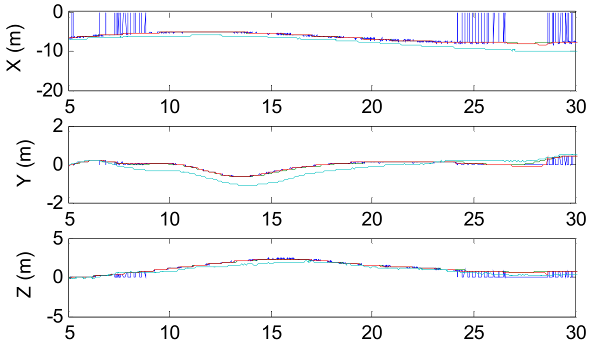

Fig. 3 Relative position

During simulations vision dropouts occurred. These can be seen when POSIT measurement goes to zero. The vertical lines indicate the beginning and end of the dropout. These vision failures can be attributed to the markers outside the tanker FOV. As can be seen, despite failures, the accuracy of the estimator remains virtually intact.

Figure 4 shows relative velocities between UAVs. The intense blue is the true data obtained from the simulator, the red one is the raw data and the green one is the estimator data.

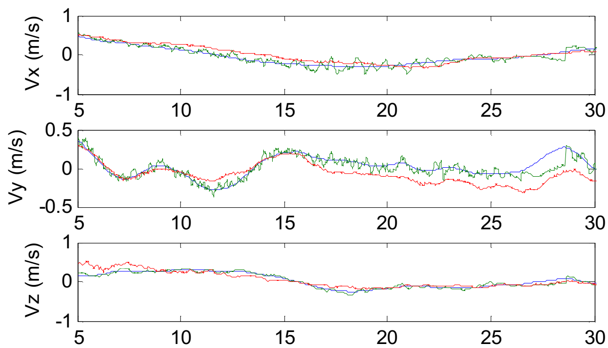

Fig. 4 Relative velocities

Figure 5 shows the boom control commands obtained from the relative state estimator, and the boom controller response. The boom controller works properly during all the refueling maneuver with an almost negligible error.

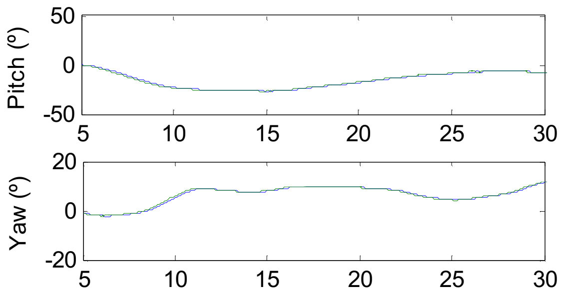

Fig. 5 Boom attitude

5 Conclusions

This paper presented the first step for an autonomous tanker UAV with a vision based estimator based in the unscented Kalman filter. Some modifications were done to enable quaternions to be used in the unscented Kalman filter. The attitude error, parametrized by GRPs was estimated for this application. A complete refueling environment was modeled, with 6dof non-linear UAV models and the boom model attached to the tanker. Simulations validated the estimator approach and demonstrated an adequate relative state estimation for the aerial refueling. The UKF based AHRS of each UAV, also demonstrated improvements. The boom controller compensates the oscillation between aircrafts. Future work will focus on real implementation, ground and flight testing, and vision system improvements to provide a robustn relative state estimation.

References

1. Mao, W., Eke, F.O.: A survey of the dynamics and control of Aircraft During Aerial Refueling. Nonlineas Dynamics and Systems Theory **8**(4), 375–388 (2008)
2. Nalepka, J.P., Hinchman, J.L.: Automated aerial refueling: extending the effectiveness of unmanned air vehicles. In: AIAA Modeling and Simulation Technologies Conference, San Francisco, CA, pp. 240–247 (2005)
3. van't Riet, R., Thomas, F.R.: KC-10A refueling boom control system. In: Proceedings of the IEEE National Aerospace and Electronics Conference, Dayton, OH, pp. 354–361 (1980)
4. Smith, J.J., Kunz, D.L.: Simulation of the dynamically coupled KC-135 tanker and refueling boom. In: 2007 AIAA Modeling and Simulation Technologies Conference, SC (2007)
5. Doebbler, J., Valasek, J., Monda, M., Schaub, H.: Boom and receptacle autonomous air refueling using a visual pressure snake optical sensor. In: AIAA Atmospheric Flight Mechanics Conference and Exhibit. American Institute of Aeronautics and Astronautics

6. Johnson, E.N., Watanabe, Y., Ha, J., Calise, A.J., Tannenbaum, A.R.: Image processing, estimation, guidance, and flight test of vision-based formation flight. In: Proceedings of the 3rd International Symposium on Innovative Aerial/Space Flyer (2006)
7. Khansari-Zadeh, S.M., Saghafi, F.: Vision-based navigation in autonomous close proximity operations using neural networks. IEEE Transactions on Aerospace and Electronic Systems **47**(2), 864–883 (2011)
8. Williamson, W.R., Glenn, G.J., Dang, V.T., Speyer, J.L., Stecko, S.M., Takacs, J.M.: Sensor fusion applied to autonomous aerial refueling. Journal of Guidance, Control, and Dynamics **32**(1), 262–275 (2009)
9. Mahboubi, Z., Kolter, Z., Wang, T., Bower, G., Ng, A.Y.: Camera based localization for autonomous UAV formation flight. In: Proceedings of the AIAA Conference (2011)
10. Julier, S.J., Uhlmann, J.K., Durrant-Whyte, H.F.: A new approach for filtering nonlinear systems. In: American Control Conference, vol. 3, pp. 1628–1632 (2012)
11. Wilson, D.B., Goktogan, A.H., Sukkarieh, S.: A vision based relative navigation framework for formation flight. In: IEEE International Conference on Robotics & Automation of the 2014, pp. 4988–4995
12. Lee, D.R., Pernicka, H.: Vision-based relative state estimation using the unscented kalman filter. International Journal of Aeronautical and Space Sciences, 24–36 (2011)
13. Rogers, R.M.: Applied Mathematics in Integrated Navigation Systems, 3rd ed., ser. AIAA Education Series. AIAA (2007)
14. Oh, S., Johnson, E.N.: Relative motion estimation for vision-based formation flight using unscented kalman filter. In: AIAA Guidance, Navigation and Control Conference and Exhibit. AIAA (2007)
15. Crassidis, J., Markley, F.: Unscented filtering for spacecraft attitude estimation. In: AIAA Guidance, Navigation, and Control Conference. AIAA
16. Dementhon, D.F., Davis, L.S.: Model-based object pose in 25 lines of code. International Journal of Computer Vision **15**(1–2), 123–141 (1995)
17. Fosbury, A., Crassidis, J.: Relative navigation of air vehicles. Journal of Guidance, Control, and Dynamics **31**(4), 824–834 (2008)